Average size of Ag nanoclusters in silica determined by optical light absorption measurements

O. Peña, L. Rodríguez-Fernández*, J. Roiz,
J.C. Cheang-Wong, J. Arenas-Alatorre, A. Crespo-Sosa, and A. Oliver
Instituto de Física, Universidad Nacional Autónoma de México,
Apartado Postal 20-364, México D.F. 01000, México.

Recibido el 7 de julio de 2006; aceptado el 7 de diciembre de 2006

Ag nanoparticles were produced in silica plates by MeV ion implantation. The mean size of the nanoclusters in the silica was determined from the optical absorption spectrum by the width of the resonant surface plasmon of the nanoparticles. The optical absorption spectrum was calculated theoretically using the classical electromagnetic Mie model considering the nanoclusters mean size information obtained experimentally. The comparisons of the experimental results with the calculations present an acceptable agreement, indicating that the Ag clusters have spherically symmetric shapes with homogenous sizes. This agreement is corroborated by transmission electron microscopy. The optical absorption method turned out to be reliable for monitoring the formation of metallic nanoparticles produced by MeV ion implantation, and allows the determination of the density of nanoclusters in the metallic phase and their mean radius.

Keywords: Nanoparticles; optical absorption; Mie theory; TEM.

Nanopartículas de Ag en una matriz de sílice se sintetizaron por medio de implantación de iones con energías del orden de MeV. El tamaño promedio de las nanopartículas se determinó a partir del espectro de absorción óptica de las muestras utilizando el ancho de la resonancia del plasmón de superficie de las partículas. Con esta información se calculó el espectro de absorción utilizando la teoría electromagnética clásica de Mie. Se compararon los espectros ópticos teóricos y experimentales y se encontró un ajuste aceptable, indicativo de que los nanocúmulos de Ag tienen formas simétricamente esféricas con tamaños homogéneos. Esto se corroboró por medio de microscopía electrónica de transmisión. Así, el método de absorción óptica resulta ser confiable para monitorear la formación de nanopartículas metálicas producidas por medio de implantación de iones con energías del orden de MeV, así como también para la determinación de la densidad de nanocúmulos en fase metálica y su radio promedio.

Descriptores: Nanopartículas; absorción óptica; teoría de Mie; TEM.

PACS: 78.70.-g; 78.67.-n; 81.07.-b; 61.82.-d

1. Introduction

Metallic nanoparticles embedded in a silica glass matrix present linear and non-linear optical properties which are very promising for technological applications in optoelectronics, such as switching devices with fast speeds and low power consumption [1,2]. However the optical properties depend on the concentration of the nanoclusters, their sizes and shapes, and their interaction with the matrix. For this reason the technological applications require reliable methods to produce these nanoparticles under controlled conditions. One of these methods is ion implantation to force the introduction of atoms into high purity silica. Ion implantation using energies of the order of MeV produce an ion depth distribution inside the matrix, some micrometers below the sample surface. This deep level ion implantation has some advantages. It is a clean method because only the selected ions are implanted. Even if some impurities can be deposited on the matrix surface, they have no effect on the nanoparticles produced deeper. Thus, the nanoparticles located underneath the surface are protected from the external media by the same matrix.

The best way to characterize the size and shape of the nanoparticles is by transmission electron microscopy (TEM). However, in the case of nanoparticles created by deep level ion implantation in silica, the major difficulty of TEM characterization is the required sample preparation. These difficulties are due to the mechanical properties of the silica matrix, the nanocluster depth distribution and the time consuming TEM sample preparation. Also, for technological applications it is not a convenient method to be used continuously in a production line. One alternative way is the characterization of the sample by optical absorption measurements. In this case, the average radius of the nanoclusters can be determined by the width of their corresponding surface plasmon resonance peak (SPR). Their symmetry can be estimated by fitting to the experimental absorption spectrum to a simulated one calculated using a theoretical model considering different shapes for the nanoclusters. The simplest exact theoretical model is due to Gustav Mie [3], and it describes the effect of light on a spherical metallic particle embedded in a dielectric medium. This model is important because it is considered as the first approximation to describe the interaction of one electromagnetic wave with small particles. In this work, Ag nanoclusters produced in high purity silica by deep level ion implantation are characterized by optical absorption spectroscopy and comparisons with simulations using the Mie Model are presented.

2. Mie theory

The Mie formulation consists in solving the classical electromagnetic equations for the interaction of a wave light with

a metallic sphere. These equations have an exact solution and a careful deduction of this solution is given by Born and Wolf [4]. Another formal solution derivation is given in Ref. 5. In general terms, the method consists of finding the solutions for the Maxwell equations in spherical polar coordinates for an incident electromagnetic plane wave impinging on a metallic sphere with a radius r embedded in a medium with refraction index n. The electromagnetic field is divided into two orthogonal subfields that can be deduced from a scalar potential. The solutions are expressed in terms of infinite series where the coefficient constants are obtained from the appropriate boundary conditions at the surface of the sphere.

The interaction of light with the sphere produces the scattering and absorption of the incident plane wave. The total energy lost from the incident wave is the sum of the scattered and absorbed energy. These energies lost are expressed in a more convenient form by the cross sections defined as the ratio between the rate of dissipation of energy and the rate at which energy is incident. The total extinction cross section σ_{ext} is given by $\sigma_{ext} = \sigma_{sca} + \sigma_{abs}$, where σ_{sca} and $\sigma_{abs}$are the scattering and absorption cross sections, respectively.

In order to express these cross sections for a metallic sphere according to the Mie formulation it is convenient to define the size parameter x and the relative refractive index m given as:

$$x = kr = \frac{2\pi nr}{\lambda} \tag{1}$$

and

$$m = \frac{n_1}{n}, \tag{2}$$

where λ is the light wavelength in vacuum and n_1 is the refraction index of the sphere. Here, k and *mk* represent the wave number in the dielectric medium and in the metallic sphere respectively. For this case the cross sections are

$$\sigma_{ext} = \frac{2\pi}{k^2}\sum_{l=1}^{\infty}(2l+1)Re\{A_l + B_l\}, \tag{3}$$

$$\sigma_{sca} = \frac{2\pi}{k^2}\sum_{l=1}^{\infty}(2l+1)(|A_l|^2 + |B_l|^2) \tag{4}$$

and

$$\sigma_{abs} = \sigma_{ext} - \sigma_{sca}. \tag{5}$$

The coefficients A_l and B_l can be calculated by the expressions

$$A_l = \frac{m\psi_l(mx)\psi_l'(x) - \psi_l(x)\psi_l'(mx)}{m\psi_l(mx)\xi_l'(x) - \xi_l(x)\psi_l'(mx)} \tag{6}$$

and

$$B_l = \frac{\psi_l(mx)\psi_l'(x) - m\psi_l(x)\psi_l'(mx)}{\psi_l(mx)\xi_l'(x) - m\xi_l(x)\psi_l'(mx)}. \tag{7}$$

The functions ψ_n and ξ_n are the Riccati-Bessel functions defined as

$$\psi_l(z) = zj_l(z) \quad \text{and} \quad \xi_l(z) = zh_l^{(1)}(z), \tag{8}$$

where $j_l(z)$ are the spherical Bessel functions and $h_l^{(1)}(z)$ the spherical Hankel functions [6, 7]. The $\psi'_l(z)$ and $\xi'_l(z)$ indicate differentiation with respect to the argument in parentheses.

This Mie solution for the extinction by a single sphere also applies to any number of spheres when they have similar diameters and they are randomly distributed with separations from each other by distances larger than the light wavelength. Under these circumstances, coherent light is not scattered by the spheres and the total scattered energy is equal to the energy scattered by one sphere multiplied by their total number. For this reason the Mie model have many practical applications.

The electron response to an electromagnetic wave in a metallic media is described by the Drude model [8], which considers that the electrons can move according to an oscillating electric field under a damping force. The solution to the corresponding electron motion equation is used to calculate the dielectric function for the media. The damping frequency involved in the solution is related to the conduction electrons interactions with their surrounding media and it can be expressed as $\omega_\gamma = v_f/\Gamma$, where v_f is the electron velocity at the Fermi level and Γ is the electron mean free path. Introducing the dielectric constant obtained by the Drude model in the Mie formulation and considering very small metallic particles, it is possible to approximate the width $\Delta\omega$ of the resonance extinction by the damping frequency with $\Gamma = r$ [9,10]. In this way, the full width at half maximum, FWHM, of the resonant band is related to the sphere radius as $\Delta\omega = v_f/r$. This expression has been used successfully in the size determination of nanoparticles into silica glass [11].

3. Experiment

The samples consisted of high-purity silica glass plates made by Nippon Silica Glass, type ED-C grade with an OH content less than 1 ppm and a total impurity content less than 20 ppm. The silica plates were implanted with 2 MeV Ag ions with a fluence of 4.8×10^{16} ions/cm^2. The ion irradiation was carried out at room temperature using the 3 MV Pelletron Tandem Accelerator at the Instituto de Física, UNAM. The ion current during the implantation was less than 0.4 μA in order to avoid thermal effects in the concentration depth distribution of the Ag ions into the silica matrix during the irradiation. The implanted samples were annealed in air at 300, 600 and 800°C. The ion depth distributions were determined by Rutherford Backscattering Spectrometry (RBS), using the same accelerator with 3 MeV $^4He^{++}$ ions.

The optical absorption measurements were obtained at room temperature using a Perkin-Elmer 300 double-beam spectrophotometer in the range 195-800 nm of wavelength. The optical properties of the nanoparticles embedded in SiO_2 are controlled mainly by the surface plasmon resonance (SPR) caused by the incident light. When the sizes of the metal nanoclusters are small compared with the wavelength

of light, their average radius r can be estimated from the SPR band using the expression $r = v_f/\Delta\omega$, where v_f is the Fermi velocity for Ag (1.39×10^8 m/s) and $\Delta\omega$ is the FWHM for the absorption band due to the SPR of the nanoclusters. The values obtained for the average radius are employed to calculate the optical extinction spectra using the classical electromagnetic theory described before. For these calculations the optical constants values for different wavelengths reported by Johnson and Christy [12] were considered.

The sample annealed at 600°C was examined by transmission electron microscopy, TEM, using a JEOL 2010F microscopy operated at 200 keV. The sample preparation was carried out using sputtering by Ar ions.

4. Results and discussion

From the RBS analysis, the Ag depth distributions into the silica glass presented a peak with a maximum concentration located at 0.91 ± 0.04 μm depth, with a FWHM of 0.4 ± 0.05 μm. No significant changes in the ion distributions are observed in the samples before and after the thermal annealing, indicating that diffusion effects are negligible during the process.

The optical absorption spectra were measured for all the samples before and after the thermal annealing. They present a very well defined SPR band at the light wavelength of 400 nm. The presence of an SPR peak for the as-implanted samples indicates the formation of Ag nanoparticles occurred during ion irradiation at room temperature. In this case, the Ag nanoclusters mean radius obtained from the measurement of the FWHM at the frequency of the SPR band was 2.81 nm. For the samples annealed at 300, 600 and 800°C, their average radii were 2.97, 3.48 and 3.20 nm, respectively.

Assuming the Ag bulk density (5.86×10^{22} atoms/cm^3) it is possible to determine the average number of atoms belonging to spherical nanoclusters in metallic phase and the cluster density in the sample as a first approximation. The clusters in the sample treated at 600°C contain the largest average number of 10350 atoms, while the average number of atoms for the as-implanted samples was 5440. Dividing the total amount of Ag atoms implanted by the average number of atoms in each particle an areal density for the clusters in the sample can be estimated. In this way, for the sample heated at 600°C it is possible to estimate an areal density of 4.64×10^{12} clusters/cm^2 and at the region of 0.91 μm depth, with higher Ag atoms concentration, the fraction of volume occupied by the nanoclusters is less than 5%.

The nanocluster sizes measured in this work have similar dimensions to the nanoparticles produced in SiO_2 by low energy ion implantation [13-15]. The difference is that the MeV energy implantation generates lower cluster density, because the implanted atoms are distributed in a larger volume. In this case, higher implantation doses are required in order to reach the same cluster density obtained by low energy implantation.

Considering the average radii measured above, the corresponding optical absorption spectrum was calculated using the Eq. (3) for the extinction cross section. Figures 1 to 4 show the comparison between the experimental and the calculated optical extinction for each sample. In general these spectra present a good agreement between the experimental and the calculated response. The best adjustment is obtained for the sample annealed at 600°C. For the other samples the experimental spectra present a shift in the position of the SPR band with respect to the calculation. These red-shifts for

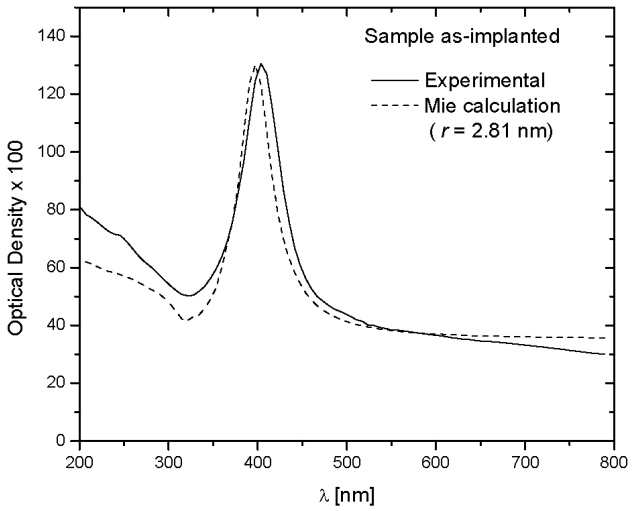

FIGURE 1. Optical extinction spectrum for an Ag as-implanted sample. The continuous line corresponds to the experimental spectrum and the dashed line to the calculated simulation using the Mie model. In parenthesis is indicated the average nanocluster radius considered for the calculation.

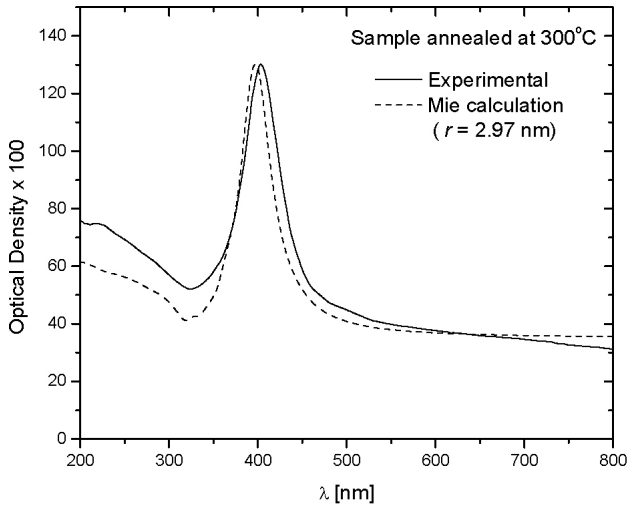

FIGURE 2. Optical extinction spectrum for the Ag implanted sample annealed at 300°C. The continuous line corresponds to the experimental spectrum and the dashed line to the calculated simulation using the Mie model. In parenthesis is indicated the average nanocluster radius considered for the calculation.

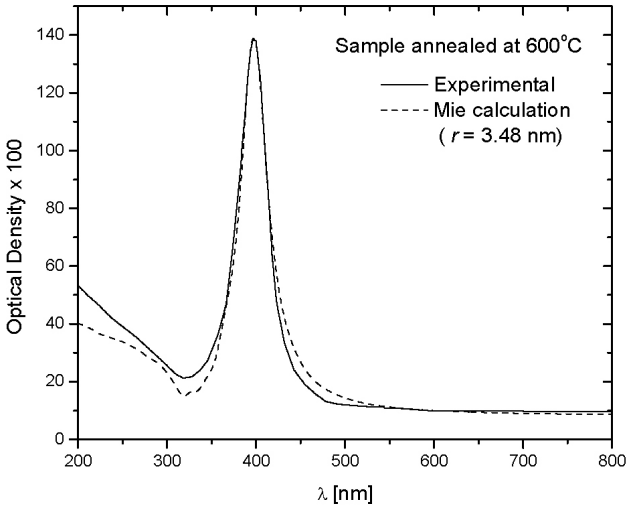

FIGURE 3. Optical extinction spectrum for the Ag implanted sample annealed at 600°C. The continuous line corresponds to the experimental spectrum and the dashed line to the calculated simulation using the Mie model. In parenthesis is indicated the average nanocluster radius considered for the calculation.

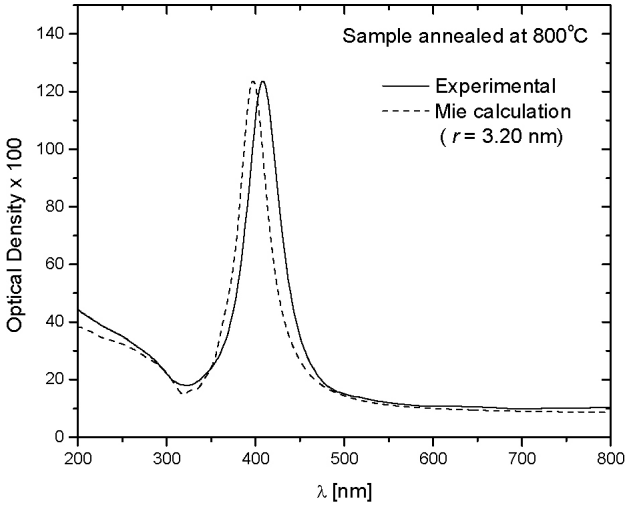

FIGURE 4. Optical extinction spectra for the Ag implanted sample annealed at 800°C. The continuous line corresponds to the experimental spectrum and the dashed line to the calculated simulation using the Mie model. In parenthesis is indicated the average nanocluster radius considered for the calculation.

the experimental spectra go from 6 nm to 14 nm and they have been observed previously [16]. As the nanocluster density obtained in the samples is small, these SPR shifts are not related to high particle concentration generating the multipoles interaction effect between the nanoparticles [15,17].

The calculations based on the Mie theory depend on the radius of the sphere and on the refraction indexes of the matrix and the metal, and is the reason why these shifts can be related to changes in the dielectric constants involved. As the refraction indexes are atomic density dependant, deviations in the atomic nanocluster structure lead to variations on these values. It is expected that for very small particles their atomic parameters can differ from those used in the calculations, corresponding to the Ag bulk material. Also, these shifts on the SPR can be related to different shapes of metallic nanoparticles. According to experimental TEM observations [18-20] and thermodynamical considerations [21], the nanoparticles actually have regular polyhedral shapes, instead of being perfect spheres.

The as-implanted and the 300°C annealed samples present the smallest size nanoclusters and their shifts of 8 nm and 6 nm respectively can be associated to this size effect on the atomic parameters. For the 600°C sample the experimental SPR peak and the calculated one are coincident. In this sample the nanoclusters are composed of the largest amount of metallic Ag atoms, producing clusters shapes closer to spheres with bulk structure. This effect can be the responsible on the SPR peaks matching.

The theoretical calculations were performed considering the total amount of Ag ions implanted (4.8×10^{16} ions/cm^2) except for the sample annealed at 800°C. For this sample a lower amount of 3.9×10^{16} ions/cm^2 Ag ions was taken into the calculation in order to match the height of the SPR band with the simulation. The intensity of the SPR band depends on the cluster amount in metallic phase and the justification to consider this decrement is because there are less Ag atoms forming metallic nanoparticles. The RBS analysis for this sample does not show any reduction in the total Ag amount implanted or any variation in its depth distribution, indicating that no loses of Ag by diffusion have taken place. However, this decrement is related to the formation of more non conductive Ag oxides which do not have the same optical response than the metallic clusters. The formation of these oxides is promoted by the annealing in the presence of air at

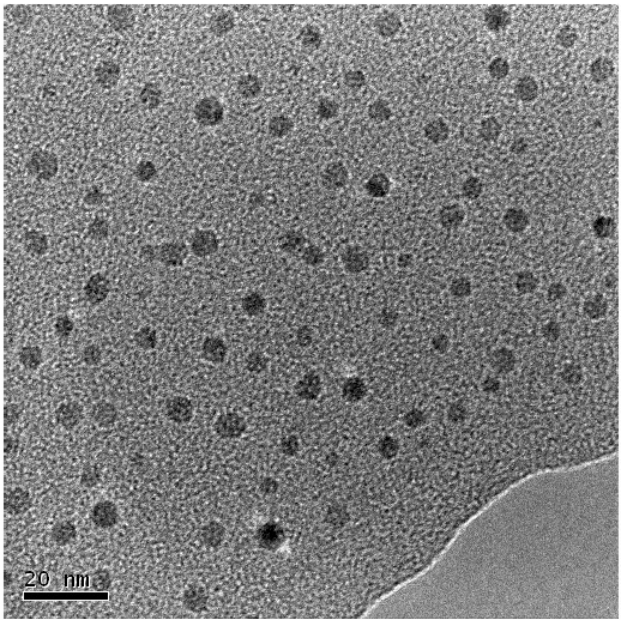

FIGURE 5. TEM image of Ag nanoclusters embedded in a high pure silica matrix implanted at 4.8×10^{16} at/cm^2, 2 MeV, for the sample annealed at 600°C in air.

800°C, where more oxygen atoms diffuse into the silica in comparison with lower temperatures. Also, the size of the metallic nanoclusters is smaller than for the sample annealed at 600°C, indicating that the nanoclusters consisted of a metallic core surrounded by an oxide shell. The presence of oxides surrounding the metallic core can alter more significantly their atomic structure parameters with respect to bulk Ag. This can be the reason why the sample at 800°C presents the major shift of 14 nm in the SPR band.

In order to corroborate the average nanocluster size obtained by the optical absorption using the Mie model, the sample annealed at 600°C was observed by TEM. Figure 5 shows the TEM image of the Ag clusters produced in this sample. The particles are not perfect spheres, but most of them have shapes spherically symmetric, and the observed nanocluster size distribution is around the same average value determined by optical absorption.

5. Conclusions

The Mie model is a first approximation to describe small particles with different shapes. Although real nanocluster can not have a perfect spherical shape [21], the general acceptable agreement between the experimental optical absorption and calculations suggest that the nanoclusters produced have spherical symmetric shapes with homogeneous sizes. Moreover, the average particles sizes determined by optical absorption are in agreement with TEM observations.

According to our results, in order to obtain the narrowest SPR band, the optimum condition is annealing the samples in air at 600°C for 1 hr. This temperature permits the formation of the largest size metallic Ag nanoclusters, homogeneous and with a spherical symmetry.

Finally, with the optical absorption method it is not possible to determine the shapes and phases of the metallic clusters, but it is possible to reaffirm the application of this nondestructive method, which is simple and fast, and capable of determining some physical properties for nanoclusters embedded into silica glasses prepared by deep level ion implantation. This is a reliable method for monitoring the formation of metallic nanoparticles, which allows the determination of the density of nanocluster in the metallic phase and their mean radius.

Acknowledgements

The authors thank to K. López and F.J. Jaimes for the accelerator operation, to J.G. Morales for the thermal annealing and TEM samples preparation, and to L. Redón for TEM manipulation. This work was supported by research grants of the UNAM-DGAPA under contract IN-119706, IN-112707, and by CONAYT under contracts U43808-F. The author O. Peña thanks to DGEP-UNAM for the scholarship provided.

∗ Contacting author: Phone: +52-55-56225160, Fax: +52-55-56225009, e-mail: luisrf@fisica.unam.mx

1. L. Pavesi, L. Dal Negro, C. Mazzoleni, G. Franzo, and F. Priolo, *Nature* **408** (2000) 440.
2. E. Borsella *et al., J. Appl. Phys.* **90** (2001) 4467.
3. G. Mie, *Ann. d. Physik* **25** (1908) 377.
4. M. Born and E. Wolf, *Principles of optics*, seven edition (Cambridge University Press, U.K., 1999).
5. C.F. Bohren and D.R. Huffman, *Absorption and scattering of light by small particles* (John Wiley & Sons, N.Y., 1983).
6. M. Abramowitz and I.A. Stegun, *Handbook of mathematical functions* (Dover Publications, Inc., N.Y., 1965).
7. G. Arfken, *Mathematical methods for physicists* (Academic Press, N.Y., 1979).
8. U. Kreibig and M. Vollmer, *Optical properties of metals clusters* (Springer-Verlag, Berlin, 1995).
9. W.T. Doyle, *Phys. Rev.* **111** (1958) 1067.
10. G.W. Arnold, *J. Appl. Phys.* **46** (1975) 4466.
11. D. Ila *et al., Nucl. Instrum. Meth. B* **141** (1998) 289.
12. P.B. Johnson and R.W. Christy, *Phys. Rev. B* **6** (1972) 4370.
13. A. Romanyuk, V. Spassov, and V. Melnik, *J. Appl. Phys.* **99** (2006) 034314.
14. M. Dubiel, H. Hofmeister, G.L. Tan, K.-D. Schicke, and E. Wendler, *Eur. Phys. J. D* **24** (2003) 361.
15. J.C. Pivin *et al., Eur. Phys. J. D* **20** (2002) 251.
16. J. Roiz *et al., J. Appl. Phys.* **95** (2004) 1783.
17. Z. Liu, H. Wang, J. Li, and X. Wang, *Appl. Phys. Let.* **72** (1998) 1823.
18. J.L. Rodríguez-López, J.M. Montejano-Carrizales, and M. José-Yacaman, *Mod. Phys. Lett. B* **20** (2006) 725.
19. J. Urban, in *Encyclopedia of Nanoscience and Nanotechnology* (Ed. by H.S. Nalwa, 2004) Vol. 10, p. 161.
20. J.M. Montejano-Carrizales *et al.*, in *Encyclopedia of Nanoscience and Nanotechnology* (Ed. by H.S. Nalwa, 2004) Vol. 2, p. 237.
21. F. Baletto and R. Ferrando, *Rev. Mod. Phys.* **77** (2005) 371.